

# Complex Antimonides with anti-Th<sub>3</sub>P<sub>4</sub> structure

A. Chamoire<sup>1</sup>, F. Gascoin<sup>1</sup>, C. Estournès<sup>2</sup>, T. Caillat<sup>3</sup> and J.-C. Tedenac<sup>1</sup>

1- Institut Charles Gerhardt Montpellier, Equipe PMOF, UMR 5253 CNRS-ENSCM-UM2-UM1, Université Montpellier II, 34095 Montpellier, France

2- CIRIMAT, PNF2 MHT, Université Paul Sabatier, 33062 Toulouse, France

3- Jet Propulsion Laboratory, California Institute of Technology, Pasadena, CA 91109, USA

Contact author: audrey.chamoire@lpmc.univ-montp2.fr

## Abstract

Polycrystalline samples of L<sub>4</sub>Sb<sub>3</sub> (L = Yb, La, Ce, Sm) and Yb<sub>4-x</sub>L'<sub>x</sub>Sb<sub>3</sub> (L' = La, Sm) have been synthesized by high temperature reaction. These compounds crystallize in the anti-Th<sub>3</sub>P<sub>4</sub> structure type (*I-43d* N°220). Powders have been characterized by X-ray diffraction and microscopic analysis, before being densified by Spark Plasma Sintering (SPS) in order to measure accurately their transport properties. Magnetic measurements show that Yb<sub>4</sub>Sb<sub>3</sub> is a mixed valence system Yb<sup>2+</sup>/Yb<sup>3+</sup>. We partially substituted Yb by trivalent rare earths elements and successfully increased the Seebeck coefficient by a factor of 2.

## Introduction

Embarked power source that does not produce CO<sub>2</sub> like thermoelectric conversion of heat, can be applied to many environmental problems. Any waste heat can be recovered and converted into electrical power. The problem of performance is crucial for this type of equipment, so the search for more efficient new materials is still a challenge.

The thermoelectric performances are estimated by the well known dimensionless

figure of merit  $ZT = \frac{\alpha^2}{\rho\kappa} T$  where  $\alpha$  is the

Seebeck coefficient,  $\rho$  the electric resistivity and  $\kappa$  the thermal conductivity which is the sum of an electronic and a lattice contribution. As  $ZT$  must be the highest possible, good thermoelectric materials must therefore combine high Seebeck coefficient, low electrical

resistivity and low thermal conductivity. Unfortunately, these three contributions are connected *via* the carrier concentration so that improving one usually degrades the others, thus limiting the  $ZT$  enhancement.

The cubic Th<sub>3</sub>P<sub>4</sub> structure (*I-43d* – N°220) and its variations (anti-Th<sub>3</sub>P<sub>4</sub> and filled Th<sub>3</sub>P<sub>4</sub>) have features that render them attractive and potentially promising candidates for thermoelectric applications.

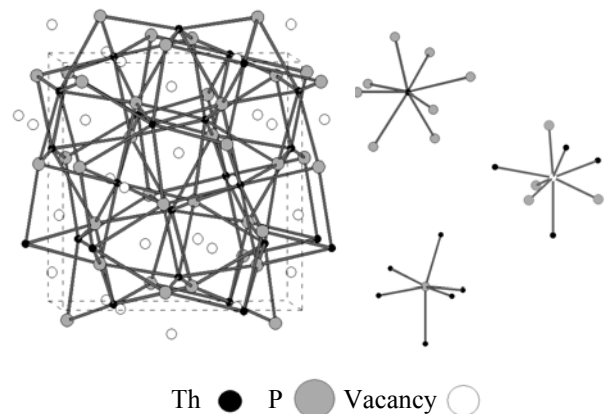


Figure 1. Cubic crystal structure of Th<sub>3</sub>P<sub>4</sub> and coordination environments of individual atoms

This structure (Figure 1) may be considered as a Zintl phase since it is an intermetallic polar phase. Thorium cation is surrounded by two interpenetrated phosphorus tetrahedra. Phosphorus anion lies in the centre of a thorium distorted octahedron and vacant site is 8-coordinated by 4 phosphorus and by 4 thorium ions forming a distorted square antiprism. Cationic sites are generally occupied by rare or alkaline earth and anionic sites by element from the columns IV, V and VI of the periodic table. Vacant sites can be filled

with a transition metal thus constituting the  $\text{Y}_3\text{Au}_3\text{Sb}_4$  structure type.

So this very complex structure has a great flexibility: it may contain several defects such as vacancies, interstitials or sites with possibility of mixed occupation that are all susceptible to reduce the lattice thermal conductivity and consequently enhanced ZT. Among  $\text{Th}_3\text{P}_4$ -type compounds we can note the n-type material  $\text{La}_{3-x}\text{Te}_4$  with a  $\text{ZT} > 1$  at 1200K [1]. We also note that antimonides, with their band structure, have proved for a long time their thermoelectric efficiency with p-type materials such as  $\text{Zn}_4\text{Sb}_3$  [2-3],  $\text{CeFe}_4\text{Sb}_{12}$  [4] or more recently  $\text{Yb}_{14}\text{MnSb}_{11}$  [5-6]. That is why we focused first on  $\text{L}_4\text{Sb}_3$  ( $\text{L} = \text{La}, \text{Ce}, \text{Sm}$  and  $\text{Yb}$ ) and more precisely on  $\text{Yb}_4\text{Sb}_3$ , and the different substitutions that can be made on anionic and/or cationic sites to improve thermoelectric properties. We present here results obtained for  $\text{Yb}_{4-x}\text{L}'_x\text{Sb}_3$  ( $\text{L}' = \text{La}$  and  $\text{Sm}$ )

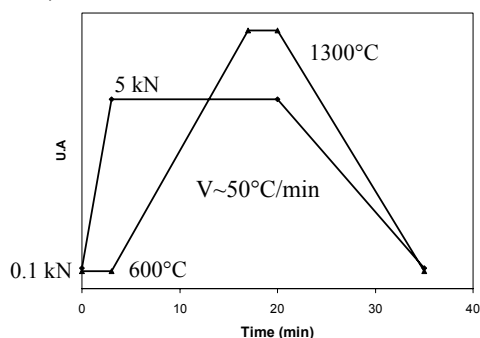


Figure 2. SPS pressure and temperature cycle as a function of time

## Experimental method

### Synthesis and characterization

$\text{L}_4\text{Sb}_3$  and  $\text{Yb}_{4-x}\text{L}'_x\text{Sb}_3$  ( $\text{L} = \text{La}, \text{Ce}, \text{Sm}$  and  $\text{Yb} - \text{L}' = \text{La}$  and  $\text{Sm}$ ) are prepared by high temperature synthesis. Stoichiometric amounts of pure elements are directly loaded into a niobium container inside a glove box. Then the container is arc welded shut under argon and in turn enclosed in a fused-silica tube under secondary vacuum ( $2-5 \cdot 10^{-6}$  mbar). These assemblies are then introduced in a tube-furnace and heated 2-4 days at  $1050^\circ\text{C}$ , before being quenched in

cold water. Then both containers are opened inside a glove box and the usually chunky material is ground before being reintroduced in new niobium and silica containers and then annealed 10 days between  $850$  and  $1000^\circ\text{C}$ .

Crystallographic analysis is made by X-rays diffraction (Philips X'Pert). Composition and microstructure are checked by electron microscopy analysis.

Powder is shaped and densified by Spark Plasma Sintering (SPS) [7] using a Dr Sinter 2080 SPS device following the cycle describe in figure 2 under a uniaxial pressure of 50MPa up to a temperature of  $1300^\circ\text{C}$ .

### Magnetic and transport properties measurements

Magnetic susceptibility is measured from 2K to room temperature using a SQUID magnetometer from Quantum Design. Electrical resistivity ( $\rho$ ) and Seebeck coefficient ( $\alpha$ ) are measured as a function of temperature (from room temperature to  $1000^\circ\text{C}$ ) on materials densified to more than 90% of the theoretical densities.

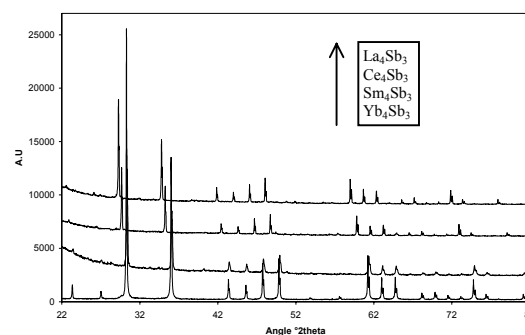


Figure 3. X-ray diffraction patterns of  $\text{L}_4\text{Sb}_3$   
 $\text{L} = \text{La}, \text{Ce}, \text{Sm}, \text{Yb}$

## Results and discussion

### Binaries $\text{L}_4\text{Sb}_3$

Binaries compounds  $\text{La}_4\text{Sb}_3$ ,  $\text{Ce}_4\text{Sb}_3$ ,  $\text{Sm}_4\text{Sb}_3$  and  $\text{Yb}_4\text{Sb}_3$  crystallize in the anti- $\text{Th}_3\text{P}_4$  structure (Figure 3) with respectively  $a = 9.649, 9.508, 9.308$  and  $9.321 \text{ \AA}$  in good agreement with previous work [8-11]. Aging studies on the four compounds show that these materials are stable in air: neither decomposition nor reaction with air occur

but only few signs of amorphization are observed on X-ray diffraction analysis after a month for  $\text{La}_4\text{Sb}_3$  and after 5 months for  $\text{Yb}_4\text{Sb}_3$ . For the other compounds no signs of amorphization are observed after 2 months. Thermogravimetric analysis confirms the thermal stability, the materials did not degrade up to  $1100^\circ\text{C}$  under inert atmosphere.

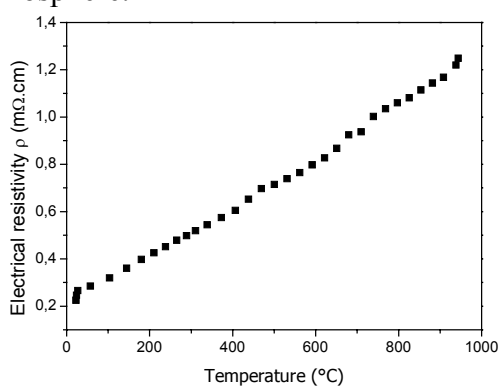


Figure 4. Resistivity of  $\text{Yb}_4\text{Sb}_3$  as a function of temperature

Molar magnetic susceptibility and transport properties measurements were only performed on polycrystalline  $\text{Yb}_4\text{Sb}_3$  ( $\chi = M/H$ , normalized per Yb). The compound does not order magnetically down to 2K, and the temperature dependence  $\chi(T)$  indicates a Curie – Weiss paramagnetic behavior. By fitting the results, we found an effective moment of  $1.87 \mu_B/\text{Yb}$ , about 41% lower than the expected value for a free  $\text{Yb}^{3+}$  ion. This indicates a mixed valence of the system. Since the electronic configuration of  $\text{Yb}^{2+}$  is  $4f^{14}$ , its total angular momentum is  $J = 0$ , and its magnetic moment  $\mu_{\text{eff}} = 0$ . Thus we can estimate the fraction of each cation considering  $\mu_{\text{eff}}(\text{Yb}^{3+}) = 4.54 \mu_B$ . The proportion of  $\text{Yb}^{2+}/\text{Yb}^{3+}$  per unit cell is 83/17, this gives a mean valence of about 2.17, value rather consistent with those estimated from ultraviolet photoemission spectroscopy [12] and from other magnetic studies performed on single crystals [13].

Transport properties are measured as a function of temperature on 95% densified “pucks”. Electrical resistivity increases linearly with temperature from about

$0.22 \text{ m}\Omega\cdot\text{cm}$  at room temperature to  $1.25 \text{ m}\Omega\cdot\text{cm}$  at  $1000^\circ\text{C}$  indicating a typical metal behavior (Figure 4). The Seebeck coefficient increases also linearly with temperature and suggests a p-type behavior from 250 up to  $1000^\circ\text{C}$  where it reaches a value of  $70 \mu\text{V}/\text{K}$ , much higher than that of a metal (Figure 5). So, these results show that  $\text{Yb}_4\text{Sb}_3$  is rather a semi-metal or a heavily doped semi-conductor. This behavior is similar to that of the most “metallic” materials from the solid solution  $\text{La}_3\text{Te}_4\text{-La}_2\text{Te}_3$  (n-type) [1]. So, this similarity allows us to think that transport properties of  $\text{Yb}_4\text{Sb}_3$  can be improved by tuning the carrier concentration.

According to our magnetic measurement and to the Zintl formalism, we can estimate that  $\text{Yb}_4\text{Sb}_3$  is electron deficient with 1.28 holes per unit cell. Therefore substitutions of Yb by a trivalent or a tetravalent rare earth like Sm, La and Ce should reduce the density of carriers.

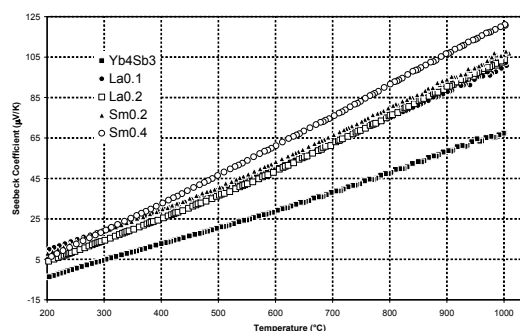


Figure 5. Resistivity of  $\text{Yb}_4\text{Sb}_3$  as a function of temperature

#### System with cationic substitute: $\text{Yb}_{4-x}\text{L}'_x\text{Sb}_3$ with $\text{L}' = \text{La}$ and $\text{Sm}$

As we can see in the X-ray diffraction pattern La can be substituted to Yb up to  $x = 0.6$  and Sm until  $x = 0.4$  without changing the structure. After reaching these limits 1/1 phases  $\text{SmSb}$  and  $\text{LaSb}$  start to be formed (Figure 6). With increasing  $x$  the lattice constant increases also from  $9.32 \text{ \AA}$  for  $\text{Yb}_{3.4}\text{La}_{0.6}\text{Sb}_3$  and to  $9.35 \text{ \AA}$  for  $\text{Yb}_{3.6}\text{Sm}_{0.4}\text{Sb}_3$ . Aging studies lead to the same conclusions made previously for binaries: compounds are stable in air and no

signs of amorphization were observed after two months.

Seebeck coefficient measurements have been performed on sample densified between 92 and 95% of the calculated theoretical densities. Figure 5 compares the Seebeck coefficient obtained with  $\text{Yb}_4\text{Sb}_3$  and partially substitute compounds  $\text{Yb}_{4-x}\text{La}_x\text{Sb}_3$  ( $x = 0.1, 0.2$ ) and  $\text{Yb}_{4-x}\text{Sm}_x\text{Sb}_3$  ( $x = 0.2, 0.4$ ). At a low value of substitution ( $x = 0.1, 0.2$ ) whatever the substituting element is (Sm or La), the Seebeck coefficient increases from 70 to  $100\mu\text{V/K}$  at  $1000^\circ\text{C}$ . For  $\text{Yb}_{3.6}\text{Sm}_{0.4}\text{Sb}_3$ ,  $\alpha$  reaches  $120\mu\text{V/K}$ , almost twice more than the initial binary.

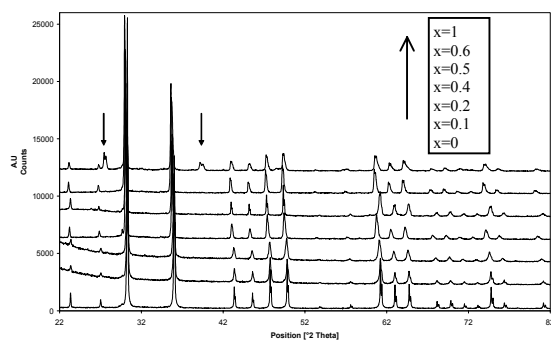


Figure 6. X-ray diffraction patterns of  $\text{Yb}_{4-x}\text{La}_x\text{Sb}_3$ , the arrows shows the  $\text{LaSb}$  phase in " $\text{Yb}_3\text{LaSb}_3$ "

As suggested, the substitution of Yb by a trivalent rare earth like La and Sm is a good mean to improve Seebeck coefficient through the lowering of the carrier concentration. Work to increase further the thermopower of such phases is underway as well as detailed electrical resistivity and thermal conductivity measurement studies. Investigations cover other type of substitutions as well as the possibilities to partially fill the interstitial sites.

## References

[1] L.R. Danielson, M.N. Alexander, C. Vining, R.A. Lockwood and C. Wood,

Seventh International Conference on Thermoelectric Energy Conversion, Arlington, Texas, March 16-18, p71 (1988).

[2] V. Izard, M.C. Record, J.C. Tedenac and S.G. Fries, *Calphad*, 25(4), p567 (2001).

[3] T. Caillat, J.-P. Fleurial, and A. Borshchevsky, *J. Phys. Chem. Solids*, 58, p1119 (1997).

[4] G. Chen, M. Dresselhaus, J.-P. Fleurial, T. Caillat, *International Materials Review*, 48 (1), p45 (2003).

[5] S. R. Brown, S.M. Kauzlarich, F. Gascoin, G.J Snyder, *Chem. Mater.*, 18, p1873, (2006).

[6] S. R. Brown, E.S. Toberer, T. Ikeda, C.A. Cox, F. Gascoin, S.M. Kauzlarich, G.J Snyder, *Chem. Mater.*, 20, p3412, (2008).

[7] C. Estournes, *Techniques de l'Ingénieur*, IN 56-1 (2006).

[8] R.J. Gambino, *J. Less-Common Met.*, 12, p344 (1967).

[9] R.E. Bodnar and H. Steinfink, *Inorg. Chem.*, 6, p327 (1967).

[10] Y. Wang, L.D. Calvert and J.B. Taylor, *Acta Cryst.*, B36, p221 (1980)

[11] A. Ochiai, S. Nakai, A. Oyamada, T. Suzuki and T. Kasuya, *J. Magn. & Magn. Mater.*, 47-48, p570 (1985).

[12] T. Mori, K. Soda, M. Yamamoto, H. Namatame, A. Ochiai, T. Suzuki, T. Kasuya and S.Suga, *J. Phys. Soc. Jpn.*, 56, p1465 (1987).

[13] S. Suga, S. Ogawa, H. Namatame, M. Tanigushi, A. Kakizaki, T. Ishii, A. Fujimori, S. Oh, H. Kato, T. Miyahara, A. Ochiai, T. Suzuki and T. Kasuya, *J. Phys. Soc. Jpn.*, 58, p4534 (1989).